Assessment of coronary flow reserve in nuclear cardiology

O. Lairez, F. Hyafil, F. Bouisset, A. Manrique, D. Agostini, F. Rouzet

Assessment of coronary flow reserve in nuclear cardiology

Évaluation de la réserve coronaire en cardiologie nucléaire

Olivier Lairez, MD, PhD [1,2]; Fabien Hyafil, MD, PhD [3] ; Frédéric Bouisset, MD [2] ; Alain Manrique, MD, PhD [4,5]; Denis Agostini, MD, PhD [4] and François Rouzet, MD, PhD [3,6]

[1]Department of Nuclear Medicine, Toulouse University Hospital, France; Cardiac Imaging Center, Toulouse University Hospital, France; Medical School, Toulouse III Paul Sabatier University, Toulouse - [2]Department of Cardiology, Rangueil University Hospital, Toulouse – [3]Department of Nuclear Medicine and DHU FIRE, Bichat-Claude Bernard Hospital, AP-HP, Paris, France; Inserm UMR 1148 and UMS 34, Paris - [4]Department of Nuclear Medicine, CHU Caen, CHU Cote de Nacre, Caen, France; Normandy University, EA 4650 Caen - [5]Cyceron PET Center, Caen - [6]University Paris-Diderot, Paris, France

Corresponding author: Olivier Lairez, MD, PhD

Department of Cardiology, Toulouse University Hospital, 1, avenue Jean Poulhès, TSA 50032, 31059 Toulouse Cedex 9

Email: lairez@gmail.com

Tel: + 33 5 61 32 28 73 - Fax: + 33 5 61 32 22 77

Abstract

The coronary flow reserve is a quantitative parameter defined by the ratio maximal myocardial blood flow to rest myocardial blood flow, which allows to give functional information on the whole coronary arterial tree, integrating both epicardial arteries and microcirculatory. The coronary flow reserve is a powerful tool to guide therapy and to assess prognosis. Exploratory tools, initially limited to experimental invasive techniques, have evolved over the last 10 years, allowing to envisage its use in daily clinical practice. This article reviews the pathophysiology of the coronary flow reserve and the various invasive and non-invasive exploration tools available to practitioners, integrating them into clinical practice.

Coronary flow reserve; myocardial blood flow; myocardial perfusion; positron emission tomography; nuclear cardiology

Résumé

La réserve coronaire est une donnée quantitative qui se définit par le ratio du flux sanguin coronaire en hyperhémie maximale sur le flux sanguin coronaire de repos, et qui permet de donner une information fonctionnelle sur l'ensemble de l'arbre artériel coronaire, à la fois épicardique et mircocirculatoire. La réserve coronaire est un outil puissant pour guider la thérapeutique et pour évaluer le pronostic. Les outils d'exploration initialement limités aux techniques invasives expérimentales ont évolué au cours des 10 dernières années permettant d'envisager une utilisation en pratique clinique quotidienne. Cet article fait une revue de la physiopathologie de la réserve coronaire et de ses différents outils d'exploration, invasifs et non invasifs, à la disposition des praticiens, en les intégrants dans la pratique clinique.

Réserve coronaire ; flux sanguin myocardique ; perfusion myocardique ; émission par émission de positons ; cardiologie nucléaire

Abbreviations

^{82}Rb: ^{82}Rubidium

CAD: coronary artery disease

CFR: coronary flow reserve

CT: computed tomography

CZT: cadmium-zinc telluride

FFR: fractional flow reserve

IMR: index of microcirculatory resistance

iwFR: instantaneous wave-free ratio

MBF: myocardial blood flow

MPI: myocardial perfusion imaging

PCI: percutaneous coronary intervention

PET: positron emission tomography

SPECT: single photon emission computed tomography

1 Pathophysiology of myocardial blood flow and coronary flow reserve

Absolute myocardial blood flow (MBF; $mL.min^{-1}.g^{-1}$) is the functional result of a dynamic arterial system composed of large epicardial coronary arteries (representing macrocirculation), prearterioles and arterioles (representing microcirculation) with different capacitance and pressure regimes [1]. Changes in MBF may reflect both macrocirculatory damage, such as stenosing coronary atheroma, as well as microcirculatory dysfunction, which is an early marker of coronary atherosclerosis and may occur in many myocardial diseases in the absence of angiographically stenosis in the epicardial arteries. There is no technique allowing for direct visualization of the coronary microcirculation *in vivo* in humans. Vessels from the coronary microcirculation have a diameter < 500 µm below the resolution of angiographic systems and are not visible on angiography. Consequently, measurement of MBF gives unique diagnostic information regarding the coronary microcirculation.

The MBF is regulated by the arteriolar tone, which allows for increasing flow via functional hyperemia when myocardial oxygen consumption increases. Because oxygen extraction from the myocardium is maximal in the resting condition, the only way to properly supply the myocardium with oxygen and fit with myocardial oxygen consumption is to modulate the coronary flow. Adenosine, which is secreted by cardiomyocytes in cases of an imbalance between myocardial oxygen supply and demand, is one of the key mediators of MBF regulation by acting on coronary arterioles [2]. Maximal hyperemic MBF (during exercise or pharmacologically induced coronary vasodilation) depends on the individual's level of training and overall clinical cardiac and general medical condition. In young healthy humans, MBF ranges from 0.7 $mL.min^{-1}.g^{-1}$ at rest up to 3 or even 4 $mL.min^{-1}.g^{-1}$ under stress, depending on the training level [3]. An absolute value of maximally stimulated (adenosine)

MBF of < 2 $mL.min^{-1}.g^{-1}$ can identify flow-limiting coronary stenosis [3] and a value < 0.91 $mL.min^{-1}.g^{-1}$ can predict the occurrence of severe life-threatening myocardial ischemia [4]. However, there is individual variation in the lower threshold value of MBF generating myocardial ischemia as a function of the workload imposed on the myocardium. Consequently, MBF values should not be used in isolation or as invariable thresholds and should be interpreted depending on the general and cardiac condition and according to the patient's level of activity.

The ratio of maximum (hyperemic) MBF to resting basal MBF is defined as the coronary flow reserve (CFR) or myocardial flow reserve, which is an integrated measure of coronary artery function through the epicardial coronary arteries to the microcirculation. The CFR represents the maximum capacity to increase coronary MBF and therefore incorporates the notion of flow “reserve”. CFR has been proposed as an indirect parameter to evaluate the function of the coronary circulation. During the ischemic process, the secretion of adenosine by the affected cardiomyocytes leads to arteriolar vasodilatation, which compensates for the MBF at rest but results in decreased CFR. Thus, CFR is the first parameter to be altered in the presence of flow-limiting coronary stenosis [5] (**Figure 1**). In patients with suspected or known coronary artery disease, CFR ≥ 2 is considered normal (3) and can reach 4 to 5 in healthy individuals [6]. However, the study of the CFR allows for an integrated exploration of the entire coronary circulation and is not limited to the epicardial coronary arteries. The CFR also integrates microcirculation and is associated with adverse cardiovascular events independent of luminal angiographic severity [7]. Because CFR is a ratio, it depends on factors that affect the level of rest or stress MBF. CFR requires measuring both rest and stress MBF. Interpreting the absolute values of rest MBF, maximal MBF and CFR can be helpful in distinguishing myocardial scar, microvascular disease or diffuse coronary artery disease (all

low rest and stress absolute MBF values) and may be useful for stratifying the prognosis. Concordant impairment of CFR and maximal MBF is associated with high cardiovascular mortality (3.3% per year), impaired CFR but preserved maximal MBF with intermediate cardiovascular mortality (1.7% per year), preserved CFR but impaired maximal MBF with low cardiovascular mortality (0.9% per year), and concordant preserved CFR and maximal MBF with the lowest cardiovascular mortality (0.4% per year) [8] (**Figure 2**). CFR and maximal MBF are indicators of the severity of coronary stenosis and microvascular function and are stronger predictors of cardiovascular mortality beyond traditional cardiovascular risk factors, left ventricular ejection fraction, myocardial scar and ischemia [8,9].

2 Non-invasive measures in nuclear cardiology

2.1 Positron emission tomography (PET)

Cardiac PET imaging has significantly evolved in the past 10 years. PET acquisitions have shifted from a 2D detection mode, in which collimators are placed in front of detectors to prevent their saturation (in particular during first-pass cardiac acquisitions), to a 3D detection mode, in which the signal can be assessed in the whole volume without any collimator needed. Acquisition of PET images in 3D mode increases the efficiency of signal detection by a factor of two [10,11]. As compared with single photon emission computed tomography (SPECT), PET technology offers accurate attenuation correction [12-14]. The spatial resolution is also increased but varies depending on averaged positron range (from 0.6 mm with ^{18}fluorine [^{18}F] to 5.9 mm with ^{82}rubidium [^{82}Rb]). Correction of photon association is based on an attenuation map extracted from a low-dose CT, which is associated with most PET systems, and translates to the possibility of reliable absolute quantification of radiotracer concentration and, using appropriate compartmental models, measurements of stress and rest myocardial blood flow [15].

2.2 ^{15}O-water

Because water diffuses freely between the blood pool and myocardium with no retention and no metabolic interactions in tissue, ^{15}O-water PET is a gold standard for non-invasive quantitative measurement of MBF [16] in that changes in myocardial activity depend on only perfusion and not flow-dependent extraction. The maximal positron energy is high (1.70 MeV), leading to an average positron range of 2.7 mm in water. However, its short half-life (2.04 min) permits sequential assessment of MBF with only modest radiation exposure to the patient (approximately 0.4 mSv for 370 MBq) [17]. Because of its linear extraction with increasing blood flow, the cut-off value for hyperaemic MBF to identify significant coronary artery disease (CAD) was reported as high as 2.50 mL.min^{-1}.g^{-1} for ^{15}O-water PET, which is much higher than the threshold range with ^{13}N-ammonia (1.15–1.85 mL.min^{-1}.g^{-1}) [18]. The high repeatability of MBF assessment allows for its use in evaluating increased MBF during the cold pressure test, a condition that generates an exclusive endothelium-dependent vasodilation and allows for non-invasive assessment of coronary endothelial function [19].

MBF as measured with ^{15}O-water PET is calculated by using the model introduced by Iida et al. [20] and is determined not from the uptake but from the washout rate of ^{15}O-water from myocardial tissue by using a single compartmental model. Because tissue attenuation affects only the height of the myocardial time–activity curve but not its shape, attenuation correction (and likely misalignment between PET and CT) may have only a modest impact on assessing myocardial flow reserve with ^{15}O-water PET [21]. However, despite its evident theoretical superiority as compared with other available tracers, the current use of ^{15}O-water remains limited to research centers with full access to a cyclotron and radiolabeled water synthesis, a situation that warrants the search for alternative fluorine-labelled perfusion tracers.

2.2 ^{82}Rubidium

^{82}Rubidium (^{82}Rb), an analog of potassium, is a PET radiotracer that accumulates in the myocardium through the Na-K-ATPase pump similar to ^{201}thallium. ^{82}Rb is taken up in viable myocardium but is rapidly cleared from fibrotic tissues. The high energy range of the emitted positron (776.5 keV) results in an intrinsic lower spatial resolution of PET images than with ^{113}N-ammonia or ^{18}F-radiolabeled tracers. ^{82}Rb can be eluted from ^{82}strontium/ ^{82}Rb generators by using an automated injector. ^{82}Rb generators are convenient for clinical use because the radiotracer can be obtained on demand just by pressing a button. Myocardial extraction of ^{82}Rb during the first-pass is high (65%) but decreases non-linearly with increasing blood flow [22]. The plateau phase at high blood flow is more pronounced than with ^{13}N-ammonia but still less marked than with ^{99m}Tc-labeled SPECT radiopharmaceuticals.

The short half-life of ^{82}Rb (75 s) translates into a high signal and low radiation exposure. Rest and stress PET acquisitions can be performed sequentially in 20 to 25 min because the injected activity of ^{82}Rb has completely decayed 7 to 8 min after injection. PET data are acquired in list mode and reconstructed into static, gated and dynamic myocardial perfusion images (**Figure 3**). In addition to the analysis of the relative myocardial perfusion and left ventricular function during stress and rest, stress and rest MBF values can be extracted from dynamic PET images by using a dedicated one-compartment model (**figure 3**).

Several studies [23-27] showed the superior diagnostic accuracy of Rb-PET-myocardial perfusion imaging (MPI) as compared with SPECT-MPI for detecting coronary stenosis > 50% because of a more reliable correction of tissue attenuation. PET acquisition during pharmacological stress also likely improves the identification of left ventricular dysfunction

provoked by balanced myocardial ischemia. Indeed, decreased left ventricular ejection fraction on stress-gated acquisitions (difference between stress and rest left ventricular ejection < 0%) is associated with high prevalence of multi-vessel CAD [26,28]. The addition of the CFR value in interpreting MPI has been found clinically relevant. A global CFR > 2.0 excludes high-risk CAD with a negative predictive value of 97% [29]. Conversely, the prevalence of multi-vessel disease is high in patients with global CFR < 1.5 and intermediate with global CFR values 1.5 to 2.0, with some overlap with microvascular disease [9,26]. In patients with estimated intermediate risk of mortality based on MPI, the addition of MFR allowed for the re-classification of 17% of patients into the high-risk group and 34% into the low-risk group [9]. CFR measurement with PET also has an important prognostic value. Symptomatic patients with normal MPI on Rb-PET have a worse prognosis if their global CFR is < 2.0 whatever the cause [30]. In addition, decreased global CFR values in 677 patients undergoing Rb-PET had a strong and incremental prognostic value over the extent of myocardial ischemia [31].

2.3 ^{13}N-ammonia

^{13}N-ammonia is synthesized on cyclotron and diffuses freely into the myocardium, where it follows various metabolic pathways. Spatial resolution of PET images is high because of the relatively low positron energy (1.19 MeV). ^{13}N-ammonia has a 10-min half-life, so a residual myocardial signal persists at the end of the PET acquisition. Thus, stress and rest PET acquisition should be separated by a 30-min interval to allow for the decay of myocardial activity, or dedicated software should be used to correct for myocardial residual activity on the second PET acquisition. ^{13}N-ammonia can be effectively used for evaluating relative myocardial uptake and left ventricular function, but image quality might be degraded because of high liver uptake or persistent lung activity in patients with decreased left ventricular

ejection fraction. ^{13}N-ammonia is mostly used for MPI in research centres owing to the relative complexity of cyclotron synthesis of the tracer and PET acquisition protocols. The metric extracted from MBF quantification with ^{13}N-ammonia-PET that correlated the best with invasive fractional flow reserve (FFR) values was relative flow reserve, the ratio between minimal MBF value in a segment and maximal MBF value in the left ventricle. A threshold value of relative flow reserve < 0.82 provided an accuracy of 83% to identify coronary stenosis with FFR < 0.80 (area under the receiver operating characteristic curve = 0.90). The number of patients imaged with ^{13}N-ammonia-PET is therefore not as large as with Rb-PET.

2.4 ^{18}F-Flurpiridaz

^{18}F-Flurpiridaz is a novel PET-MPI tracer labeled with ^{18}F that binds to mitochondrial complex 1. Preclinical studies demonstrated that flurpiridaz has high myocardial extraction and prolonged retention. Because of the relatively longer decay of ^{18}F as compared with the currently available PET tracers, flurpiridaz may be produced as a unit dose from a regional cyclotron, thus obviating the need for an on-site cyclotron or generator [22,23]. Phase 1 flurpiridaz studies [24,25] have shown that this tracer is clinically safe, has acceptable clinical dosimetry, and provides high-quality images in conjunction with exercise treadmill testing as well as pharmacological coronary vasodilation stress testing.

3 New tools using single photon emission CT

Cadmium-zinc telluride (CZT) SPECT camera systems have higher photon sensitivity than conventional Anger camera systems [32,33], which allows for MBF measurements from early dynamic acquisitions [34-40].

3.1 Dynamic ^{99m}Tc-sestamibi CZT-SPECT acquisition protocol

Rest and stress dynamic images are acquired in list mode over 6 min. For rest imaging, approximately 37 MBq of ^{99m}Tc-sestamibi is used to position the patient's heart within the field of view [37]. Next, 3 MBq.kg^{-1} is injected at a rate of 1 to 2 ml.s^{-1} by using an automatic injector. For stress imaging, 9 MBq.kg^{-1} of ^{99m}Tc-sestamibi is injected after the administration of regadenoson (400 μg). Rest–stress dynamic acquisitions are usually completed within 75 min.

3.2 MBF quantification by dynamic ^{99m}Tc-sestamibi CZT-SPECT

A global myocardial region of interest is placed semi-automatically to obtain the myocardial time activity curves from the summed dynamic image data, starting 2 min after the last frame images of the dynamic SPECT data. The ^{99m}Tc-sestamibi model uses a one-tissue compartment model with k2 set to 0 (equivalent to net retention model) with blood-to-myocardium spillover fraction and myocardial partial-volume corrections [41]. MBF is obtained by correcting the K1 values for the flow-dependent extraction fraction based on the model by Leppo et al. [41]. Regional analysis is performed with standardized myocardial wall segmentation for the left anterior descending, left circumflex and right coronary artery (**Figure 4**).

Multiple reports have demonstrated the feasibility of SPECT MBF quantification [34-39,42]. Two studies have performed head-to head comparisons between SPECT with a CZT camera system and PET. Nkoulo et al. studied 28 patients who underwent ^{99m}Tc-tetrofosmin CZT SPECT and ^{13}N-ammonia PET [38]. The authors showed moderate correlation, assessed using Spearman's correlation, between SPECT and PET for measurements. Stress MBF was

underestimated by SPECT at high flow conditions, which resulted in underestimating MFR. However, the authors did not correct for the extraction fraction of ^{99m}Tc, which is a significant limitation of SPECT MBF measurements, particularly at high flow. The WATERDAY study compared MBF quantification between ^{99m}Tc-sestamibi CZT SPECT and ^{15}O-water PET. The study demonstrated good correlation for MBF and CFR between SPECT and PET by using Corridor 4DM software (INVIA, Ann Arbor, MI, USA) [36]. In contrast to results from Nkoulo et al., global stress MBF by ^{99m}Tc-sestamibi CZT SPECT was higher than ^{15}O-water PET values.

Agostini et al. found higher SPECT MBF values at rest and stress in the left anterior descending and left circumflex territories but not the right coronary artery [36]. With CZT SPECT camera systems, attenuation artifacts are more common in the inferolateral and lateral wall, which may affect MBF measurements in these territories.

4 Invasive approach

4.1 FFR

The FFR is an invasive procedure that can be used during coronary angiography to determine the functional impact of an epicardial coronary stenosis and was introduced by Pijls et al. in 1993 [43]. It can be used for patients with stable CAD or to assess non-culprit lesions in acute coronary syndrome. In the context of stable CAD, performing a coronary revascularisation by percutaneous coronary intervention (PCI) on the basis of angiographic appreciation of a stenosis does not provide significant benefit to the patient as compared with an optimal medical treatment alone, according to the COURAGE trial [44]. This observation is probably due at least in part to the poor correlation between angiographical degree of stenosis and

ischemia [45]. Hence, FFR appears particularly relevant when no functional tests have been performed before coronary angiography.

4.2 FFR principle

By definition, the FFR represents the ratio between the pressure measured distal to a coronary stenosis (Pd) obtained on maximal hyperaemia and the aortic pressure (Pa). Thus, FFR is measured by advancing a dedicated pressure wire within the coronary artery, behind the coronary stenosis, to measure the Pd value. The Pa value is measured at the extremity on the catheter placed in the coronary ostia. Maximal coronary hyperaemia is then obtained by injecting a vasodilator, in most cases adenosine, directly in the coronary artery or intravenously via a central venous line. Hence, the maximal possible FFR value is 1 and denotes the absence of epicardial coronary stenosis. In case of coronary stenosis, the FFR value decreases (**Figure 5**). A value > 0.8 is considered abnormal and can justify revascularisation (interventional or surgical), if appropriate.

4.3 Main randomised clinical trials

The first major randomised clinical trial of FFR was the DEFER study, reported in 2001 [46]. This study demonstrated that angiographically moderate stenosis with a normal FFR value had good prognosis, with no benefit of angioplasty. The second major trial was the FAME study, reported in 2009 [47], which showed that FFR-guided PCI performed better than angio-guided PCI, involved fewer stents and reduced the rate of death and myocardial infarction at 1-year follow-up. Finally, the FAME II study published in 2012 [48] demonstrated that PCI treatment of stenosis with a pathological FFR value (> 0.8) reduced the 1-year rate of a composite criteria including death, myocardial infarction and urgent revascularisation. Of note, the positive findings from this trial were mainly driven by reduced

need for urgent revascularisation. However, the results at 5 years, recently published [49], showed a significant reduction in rate of myocardial infarction, which confirms the interest of this technique, with a benefit on a hard endpoint.

4.4 Instantaneous wave-free ratio (iwFR)

iwFR is an alternative invasive pressure-based coronary physiological index introduced in 2012 [50] that does not require pharmacological hyperemia. The absence of hyperemia reduces both the measurement time and the patient's discomfort. The iwFR is obtained, as for FFR, by using a pressure wire advanced distal to the coronary stenosis. The iwFR is estimated by calculating the ratio (Pd/Pa) between the pressure assessed in the coronary artery distal to the stenosis (Pd) and the pressure in the aorta (Pa). This ratio is calculated by use of dedicated programs during a specific period in diastole, called the wave-free period. This technique was compared to the FFR (technique of reference) in two large randomized controlled trials and was found non-inferior [51,52]. As a result, to date, iwFR has the same level of recommendation as FFR in the latest European Society of Cardiology (ESC) Guidelines (Class I, level A) [53].

4.5 Index of microcirculatory resistance

Although the microcirculation represents 90% to 95% of the coronary tree, its direct visualization during traditional coronary angiography is impossible. Several methods have been proposed to explore the microcirculation. The simplest invasive ways to assess microcirculation, mainly used in the setting of ST-elevation myocardial infarction, are the TIMI flow and the myocardial blush. However, these methods are highly subjective. The FFR value integrates the microcirculation — two similar stenoses can have different FFR values depending on the underlying microcirculatory bed — but does not constitute by itself an index

to measure microcirculation. Similarly, the CFR, defined as the ratio between maximum and resting MBF, interrogates the overall coronary circulation and has major limitations in the assessment of microcirculation. Indeed, this measure has high variability and provides a global result with no distinction between the respective parts of the epicardial vessel and microvasculature in case of pathological result.

The index of microcirculatory resistance (IMR) measures the resistance to myocardial flow, specifically related to the coronary microcirculation compartment. This index, described in 2003 [54], is defined as the ratio of distal coronary pressure (Pd) and the thermodilution-derived mean transit time during maximal hyperemia, measured with a pressure/temperature wire or microcatheter. This index, specific to the microvasculature, has low variability and superior reproducibility to CFR [55]. It is of particular interest in case of suspected coronary microvascular angina or when a patient presents an abnormal stress study and angina but has no significant epicardial coronary disease. In the recent ESC guidelines for chronic coronary syndrome [53], this tool is recommended to assess patients who are symptomatic despite an angiographically normal or sub-normal coronary artery (Class IIA, level B). In the setting of ST-elevation myocardial infarction, a high IMR value (> 40, normal value is < 25) assessed in the culprit artery after pathological percutaneous coronary angioplasty is strongly and independently associated with the occurrence of death or rehospitalization for heart failure because it identifies patients who have not achieved successful reperfusion of the microvasculature despite epicardial coronary angioplasty.

5 Alternative approaches in non-invasive imaging

5.1 Transthoracic echocardiography

By allowing coronary flow velocity measurements, transthoracic echocardiography was used in the late 1990s [56] to explore maximal coronary vasodilator capacity and CFR as indicators of coronary stenosis severity and microvascular function. The technique is based on measuring coronary flow velocity at rest and after maximally stimulated vasodilatation in the distal left anterior descending coronary artery by using transthoracic echocardiography under the guidance of color Doppler flow mapping with a high-frequency transducer. The technique has shown good correlation with invasive measurements [57] with several limitations due to the acoustic window, the variability of the results with the positioning of the wire and the difficulties in exploring tortuous segments and regions with varying luminal dimensions or configurations in echocardiography but also the limited nature of left anterior descending coronary artery exploration alone.

5.2 Magnetic resonance imaging (MRI)

Absolute quantification of MBF by MRI is challenging, and perfusion cardiac MRI is most commonly evaluated qualitatively. With the difficulties in obtaining accurate quantification of MBF due to the lack of linearity between the measured signal and contrast agent concentration, early MRI works focused on quantifying venous outflow in the distal coronary sinus [58] or coronary flow in the left anterior descending coronary artery [59] by using phase velocity mapping sequences at rest and after maximally stimulated vasodilatation. However, these methods were limited because of the large movement of the coronary sinus and the coronary arteries during the cardiac cycle, so accurate quantification of the flow was challenging.

New dual sequence approaches, optimizing the imaging protocols for blood and myocardium perfusion quantification are in progress [60], but the most promise perspective probably comes from free contrast-agent T1 mapping sequences, which are highly sensitive to changes in myocardial water content, thereby allowing to detect changes in myocardial blood volume at rest and during vasodilatory stress [61].

5.3 FFR by CT

Non-invasive anatomic assessment of coronary arteries by coronary CT angiography is being increasingly used for detecting or excluding CAD. However, despite good negative predictive value, the technique remains limited by a purely morphological approach that does not allow for evaluating the hemodynamic impact of the lesion. Recently, methods involving computational fluid dynamics from coronary CT angiography (FFR_{CT}) to calculate coronary blood flow, pressure, and FFR have been developed [62-64]. These methods use routinely acquired coronary CT angiography datasets and calculate the hemodynamic impact of lesions by modeling resting coronary flow from arterial pressure data. FFR_{CT} provides high diagnostic accuracy and discrimination for the diagnosis of hemodynamically significant CAD, with invasive FFR as the reference standard [65]. However, this new technique models arterial flow on the basis of an epicardial coronary lesion and therefore does not allow for exploring microcirculation, which in the absence of direct visualization, requires exploring coronary flow during vasodilatory stress.

6 Interest of coronary flow reserve over standard MPI

The added value of direct measurement of CFR in addition to MPI relies on two aspects: diagnosis and prognosis. The first relates to the false negative results occurring when 3-vessel

coronary stenosis results in balanced ischemia with reduced but homogeneous distribution of the perfusion tracer. The ability to demonstrate the absence or a blunted increase in MBF after coronary vasodilation allows the diagnosis to be corrected [66]. The prognostic value is by far the most promising. It is now clear that CFR enables prognostic reclassification in patients with suspected or proven CAD, above traditional risk factors such as the Framingham risk score, but also left ventricular ejection fraction, anti-anginal drugs, and even the presence and extent of myocardial ischemia and/or scar. Because coronary blood flow and flow reserve depend on both the epicardial segment of coronary arteries and microcirculation [1], the risk evidenced by CFR seems to integrate all the separate risk factors in one parameter, with a resulting hazard ratio far above all others [9]. A practical application of such risk stratification has been demonstrated in a large population. In this study, among diabetic patients without known CAD, those with preserved CFR (>1.6) presented an annual event rate similar to non-diabetic and non-CAD patients, whereas in those with CFR ≤1.6, the annual event rate was comparable to diabetic patients with a history of CAD [67]. This integrative risk stratification is particularly relevant at a time when the benefit of revascularization in patients with stable CAD (also called chronic coronary syndromes in the recent ESC recommendations [53]) is much debated, with no evidence of impact on mortality. Of note, a recent survey performed in >12,000 patients who underwent ^{82}Rubidium PET for suspected or known CAD showed that CFR was able to identify those who received a survival benefit with early revascularization compared to medical therapy [68] Also, an accurate evaluation of the cardiovascular risk could serve as an endpoint to adjust management of risk factors by lifestyle changes and medicine.

7 Limits of application of MBF measurement using nuclear cardiology in clinical practice

Despite the interest in measuring MBF and CFR in clinical practice, their realization in clinical practice is still limited. The authorization for use and reimbursement of PET tracers for measuring coronary perfusion varies among countries and in all cases is hampered by the half-life of the tracer, which requires the use of a generator in the best case or a cyclotron in the worst case, for an expensive technique. The problem of accessibility, authorizations and price is not the same in SPECT with CZT cameras and ^{99m}Tc tracers, which explains the growing interest in the latter modality [68].

In all cases, image reconstruction and processing require dedicated tools, and to date, stress protocols are limited to pharmacological stress due to the impossibility of performing dynamic acquisition during effort. Hence, the advantages and added value of coronary flow quantification can be counterbalanced by the loss of information and diagnostic performance due to physiological stress during exercise.

8 Conclusions

The measurement of MBF and CFR allows for going beyond the anatomical exploration of coronary arteries, which is limited to the macro-circulation, to provide functional information on the entire vascular tree, including micro-circulation. This comprehensive, non-invasive, quantitative and physiological approach to coronary circulation allows for guiding the therapeutic decision and assessing the burden of the disease and associated prognosis. Although the accessibility of PET tracers is still limited in clinical practice, the widespread

availability of CZT-SPECT cameras, allowing for dynamic acquisition, allows for considering the use of the technique in routine daily practice.

References

1. Camici PG, Rimoldi OE. The clinical value of myocardial blood flow measurement. J. Nucl. Med. 2009;50:1076–87.

2. Belardinelli L, Linden J, Berne RM. The cardiac effects of adenosine. Prog. Cardiovasc. Dis. 1989;32:73–97.

3. Gewirtz H, Dilsizian V. Integration of Quantitative Positron Emission Tomography Absolute Myocardial Blood Flow Measurements in the Clinical Management of Coronary Artery Disease. Circulation 2016;133:2180–96.

4. Johnson NP, Gould KL. Physiological basis for angina and ST-segment change PET-verified thresholds of quantitative stress myocardial perfusion and coronary flow reserve. JACC. Cardiovasc. Imaging 2011;4:990–8.

5. Detry JM. The pathophysiology of myocardial ischaemia. Eur. Heart J. 1996;17 Suppl G:48–52.

6. Sdringola S, Johnson NP, Kirkeeide RL, Cid E, Gould KL. Impact of unexpected factors on quantitative myocardial perfusion and coronary flow reserve in young, asymptomatic volunteers. JACC. Cardiovasc. Imaging 2011;4:402–12.

7. Taqueti VR, Hachamovitch R, Murthy VL, et al. Global coronary flow reserve is associated with adverse cardiovascular events independently of luminal angiographic severity and modifies the effect of early revascularization. Circulation 2015;131:19–27.

8. Gupta A, Taqueti VR, van de Hoef TP, et al. Integrated Noninvasive Physiological Assessment of Coronary Circulatory Function and Impact on Cardiovascular Mortality in Patients With Stable Coronary Artery Disease. Circulation 2017;136:2325–36.

9. Murthy VL, Naya M, Foster CR, et al. Improved cardiac risk assessment with noninvasive measures of coronary flow reserve. Circulation 2011;124:2215–24.

10. Schepis T, Gaemperli O, Treyer V, et al. Absolute quantification of myocardial blood flow with 13N-ammonia and 3-dimensional PET. J. Nucl. Med. 2007;48:1783–9.

11. Knesaurek K, Machac J, Krynyckyi BR, Almeida OD. Comparison of 2-dimensional and 3-dimensional 82Rb myocardial perfusion PET imaging. J. Nucl. Med. 2003;44:1350–6.

12. Yoshinaga K, Chow BJW, Williams K, et al. What is the prognostic value of myocardial perfusion imaging using rubidium-82 positron emission tomography? J. Am. Coll. Cardiol. 2006;48:1029–39.

13. Sampson UK, Dorbala S, Limaye A, Kwong R, Di Carli MF. Diagnostic accuracy of rubidium-82 myocardial perfusion imaging with hybrid positron emission tomography/computed tomography in the detection of coronary artery disease. J. Am. Coll. Cardiol. 2007;49:1052–8.

14. Freedman N, Schechter D, Klein M, Marciano R, Rozenman Y, Chisin R. SPECT attenuation artifacts in normal and overweight persons: insights from a retrospective

comparison of Rb-82 positron emission tomography and TI-201 SPECT myocardial perfusion imaging. Clin. Nucl. Med. 2000;25:1019–23.

15. Schindler TH, Quercioli A, Valenta I, Ambrosio G, Wahl RL, Dilsizian V. Quantitative assessment of myocardial blood flow--clinical and research applications. Semin. Nucl. Med. 2014;44:274–93.

16. Knaapen P. Quantitative myocardial blood flow imaging: not all flow is equal. Eur. J. Nucl. Med. Mol. Imaging 2014;41:116–8.

17. Stabin MG. Radiopharmaceuticals for nuclear cardiology: radiation dosimetry, uncertainties, and risk. J. Nucl. Med. 2008;49:1555–63.

18. Gould KL, Johnson NP, Bateman TM, et al. Anatomic versus physiologic assessment of coronary artery disease. Role of coronary flow reserve, fractional flow reserve, and positron emission tomography imaging in revascularization decision-making. J. Am. Coll. Cardiol. 2013;62:1639–53.

19. Legallois D, Belin A, Nesterov S V, et al. Cardiac rehabilitation improves coronary endothelial function in patients with heart failure due to dilated cardiomyopathy: A positron emission tomography study. Eur. J. Prev. Cardiol. 2016;23:129–36.

20. Iida H, Rhodes CG, de Silva R, et al. Use of the left ventricular time-activity curve as a noninvasive input function in dynamic oxygen-15-water positron emission tomography. J. Nucl. Med. 1992;33:1669–77.

21. Tuffier S, Legallois D, Belin A, et al. Assessment of endothelial function and myocardial flow reserve using (15)O-water PET without attenuation correction. Eur. J. Nucl. Med. Mol. Imaging 2016;43:288–95.

22. Goldstein RA, Mullani NA, Marani SK, Fisher DJ, Gould KL, O'Brien HAJ. Myocardial perfusion with rubidium-82. II. Effects of metabolic and pharmacologic interventions. J. Nucl. Med. 1983;24:907–15.

23. Bateman TM, Heller G V, McGhie AI, et al. Diagnostic accuracy of rest/stress ECG-gated Rb-82 myocardial perfusion PET: comparison with ECG-gated Tc-99m sestamibi SPECT. J. Nucl. Cardiol. 2006;13:24–33.

24. Go RT, Marwick TH, MacIntyre WJ, et al. A prospective comparison of rubidium-82 PET and thallium-201 SPECT myocardial perfusion imaging utilizing a single dipyridamole stress in the diagnosis of coronary artery disease. J. Nucl. Med. 1990;31:1899–1905.

25. Stewart RE, Schwaiger M, Molina E, et al. Comparison of rubidium-82 positron emission tomography and thallium-201 SPECT imaging for detection of coronary artery disease. Am. J. Cardiol. 1991;67:1303–10.

26. Hyafil F, Chequer R, Sorbets E, et al. Head-to-head comparison of the diagnostic performances of Rubidium-PET and SPECT with CZT camera for the detection of myocardial ischemia in a population of women and overweight individuals. J. Nucl. Cardiol. 2018. doi: 10.1007/s12350-018-01557-z. [Epub ahead of print]

27. Hyafil F, Chequer R, Rouzet F, et al. La TEP au 82-Rubidium permet une meilleure détection des patients tri-tronculaires comparativement à la SPECT avec caméras CZT. Médecine Nucléaire 2018;42:141.

28. Dorbala S, Vangala D, Sampson U, Limaye A, Kwong R, Di Carli MF. Value of vasodilator left ventricular ejection fraction reserve in evaluating the magnitude of myocardium at risk and the extent of angiographic coronary artery disease: a 82Rb PET/CT study. J. Nucl. Med. 2007;48:349–58.

29. Naya M, Murthy VL, Taqueti VR, et al. Preserved coronary flow reserve effectively excludes high-risk coronary artery disease on angiography. J. Nucl. Med. 2014;55:248–55.

30. Naya M, Murthy VL, Foster CR, et al. Prognostic interplay of coronary artery calcification and underlying vascular dysfunction in patients with suspected coronary artery disease. J. Am. Coll. Cardiol. 2013;61:2098–2106.

31. Ziadi MC, Dekemp RA, Williams KA, et al. Impaired myocardial flow reserve on rubidium-82 positron emission tomography imaging predicts adverse outcomes in patients assessed for myocardial ischemia. J. Am. Coll. Cardiol. 2011;58:740–8.

32. Sharir T, Ben-Haim S, Merzon K, et al. High-speed myocardial perfusion imaging initial clinical comparison with conventional dual detector anger camera imaging. JACC. Cardiovasc. Imaging 2008;1:156–63.

33. Imbert L, Poussier S, Franken PR, et al. Compared performance of high-sensitivity cameras dedicated to myocardial perfusion SPECT: a comprehensive analysis of phantom and human images. J. Nucl. Med. 2012;53:1897–1903.

34. Ben-Haim S, Murthy VL, Breault C, et al. Quantification of Myocardial Perfusion Reserve Using Dynamic SPECT Imaging in Humans: A Feasibility Study. J. Nucl. Med. 2013;54:873–9.

35. Wells RG, Marvin B, Poirier M, Renaud J, deKemp RA, Ruddy TD. Optimization of SPECT Measurement of Myocardial Blood Flow with Corrections for Attenuation, Motion, and Blood Binding Compared with PET. J. Nucl. Med. 2017;58:2013–9.

36. Agostini D, Roule V, Nganoa C, et al. First validation of myocardial flow reserve assessed by dynamic (99m)Tc-sestamibi CZT-SPECT camera: head to head comparison with (15)O-water PET and fractional flow reserve in patients with suspected coronary artery disease. The WATERDAY study. Eur. J. Nucl. Med. Mol. Imaging 2018;45:1079–90.

37. Bellevre D, Manrique A, Legallois D, et al. First determination of the heart-to-mediastinum ratio using cardiac dual isotope ((1)(2)(3)I-MIBG/(9)(9)mTc-tetrofosmin) CZT imaging in patients with heart failure: the ADRECARD study. Eur. J. Nucl. Med. Mol. Imaging 2015;42:1912–9.

38. Nkoulou R, Fuchs TA, Pazhenkottil AP, et al. Absolute Myocardial Blood Flow and Flow Reserve Assessed by Gated SPECT with Cadmium-Zinc-Telluride Detectors Using 99mTc-Tetrofosmin: Head-to-Head Comparison with 13N-Ammonia PET. J. Nucl. Med. 2016;57:1887–92.

39. Han S, Kim Y-H, Ahn J-M, et al. Feasibility of dynamic stress (201)Tl/rest (99m)Tc-tetrofosmin single photon emission computed tomography for quantification of myocardial perfusion reserve in patients with stable coronary artery disease. Eur. J. Nucl. Med. Mol. Imaging 2018;45:2173–80.

40. James C, Guineau C, Leprovost M, et al. Évaluation quantitative de la réserve coronaire par étude dynamique sous caméra-CZT : méthodologie et aspects pratiques. Médecine Nucléaire 2016;40:182–3.

41. Leppo JA, Meerdink DJ. Comparison of the myocardial uptake of a technetium-labeled isonitrile analogue and thallium. Circ. Res. 1989;65:632–9.

42. Ben Bouallegue F, Roubille F, Lattuca B, et al. SPECT Myocardial Perfusion Reserve in Patients with Multivessel Coronary Disease: Correlation with Angiographic Findings and Invasive Fractional Flow Reserve Measurements. J. Nucl. Med. 2015;56:1712–7.

43. Pijls NH, van Son JA, Kirkeeide RL, De Bruyne B, Gould KL. Experimental basis of determining maximum coronary, myocardial, and collateral blood flow by pressure measurements for assessing functional stenosis severity before and after percutaneous transluminal coronary angioplasty. Circulation 1993;87:1354–67.

44. Boden WE, O'Rourke RA, Teo KK, et al. Optimal medical therapy with or without PCI for stable coronary disease. N. Engl. J. Med. 2007;356:1503–16.

45. Tonino PAL, Fearon WF, De Bruyne B, et al. Angiographic versus functional severity of coronary artery stenoses in the FAME study fractional flow reserve versus angiography in multivessel evaluation. J. Am. Coll. Cardiol. 2010;55:2816–21.

46. Bech GJ, De Bruyne B, Pijls NH, et al. Fractional flow reserve to determine the appropriateness of angioplasty in moderate coronary stenosis: a randomized trial. Circulation 2001;103:2928–34.

47. Tonino PAL, De Bruyne B, Pijls NHJ, et al. Fractional flow reserve versus angiography for guiding percutaneous coronary intervention. N. Engl. J. Med. 2009;360:213–24.

48. De Bruyne B, Pijls NHJ, Kalesan B, et al. Fractional flow reserve-guided PCI versus medical therapy in stable coronary disease. N. Engl. J. Med. 2012;367:991–1001.

49. Xaplanteris P, Fournier S, Pijls NHJ, et al. Five-Year Outcomes with PCI Guided by Fractional Flow Reserve. N. Engl. J. Med. 2018;379:250–9.

50. Sen S, Escaned J, Malik IS, et al. Development and validation of a new adenosine-independent index of stenosis severity from coronary wave-intensity analysis: results of the ADVISE (ADenosine Vasodilator Independent Stenosis Evaluation) study. J. Am. Coll. Cardiol. 2012;59:1392–1402.

51. Davies JE, Sen S, Dehbi H-M, et al. Use of the Instantaneous Wave-free Ratio or Fractional Flow Reserve in PCI. N. Engl. J. Med. 2017;376:1824–34.

52. Gotberg M, Christiansen EH, Gudmundsdottir IJ, et al. Instantaneous Wave-free Ratio versus Fractional Flow Reserve to Guide PCI. N. Engl. J. Med. 2017;376:1813–23.

53. Knuuti J, Wijns W, Saraste A, et al. 2019 ESC Guidelines for the diagnosis and management of chronic coronary syndromes. Eur. Heart J. 2020;41:407-77.

54. Fearon WF, Balsam LB, Farouque HMO, et al. Novel index for invasively assessing the coronary microcirculation. Circulation 2003;107:3129–32.

55. Ng MKC, Yeung AC, Fearon WF. Invasive assessment of the coronary microcirculation: superior reproducibility and less hemodynamic dependence of index of microcirculatory resistance compared with coronary flow reserve. Circulation 2006;113:2054–61.

56. Hozumi T, Yoshida K, Ogata Y, et al. Noninvasive assessment of significant left anterior descending coronary artery stenosis by coronary flow velocity reserve with transthoracic color Doppler echocardiography. Circulation 1998;97:1557–62.

57. Hozumi T, Yoshida K, Akasaka T, et al. Noninvasive assessment of coronary flow velocity and coronary flow velocity reserve in the left anterior descending coronary artery by Doppler echocardiography: comparison with invasive technique. J. Am. Coll. Cardiol. 1998;32:1251–9.

58. van Rossum AC, Visser FC, Hofman MB, Galjee MA, Westerhof N, Valk J. Global left ventricular perfusion: noninvasive measurement with cine MR imaging and phase velocity mapping of coronary venous outflow. Radiology 1992;182:685–91.

59. Davis CP, Liu PF, Hauser M, Gohde SC, von Schulthess GK, Debatin JF. Coronary flow and coronary flow reserve measurements in humans with breath-held magnetic resonance phase contrast velocity mapping. Magn. Reson. Med. 1997;37:537–44.

60. Kellman P, Hansen MS, Nielles-Vallespin S, et al. Myocardial perfusion cardiovascular magnetic resonance: optimized dual sequence and reconstruction for quantification. J. Cardiovasc. Magn. Reson. 2017;19:43.

61. Liu A, Wijesurendra RS, Francis JM, et al. Adenosine Stress and Rest T1 Mapping Can Differentiate Between Ischemic, Infarcted, Remote, and Normal Myocardium Without the Need for Gadolinium Contrast Agents. JACC. Cardiovasc. Imaging 2016;9:27–36.

62. Koo B-K, Erglis A, Doh J-H, et al. Diagnosis of ischemia-causing coronary stenoses by noninvasive fractional flow reserve computed from coronary computed tomographic angiograms. Results from the prospective multicenter DISCOVER-FLOW (Diagnosis of Ischemia-Causing Stenoses Obtained Via Noni. J. Am. Coll. Cardiol. 2011;58:1989–97.

63. Min JK, Leipsic J, Pencina MJ, et al. Diagnostic accuracy of fractional flow reserve from anatomic CT angiography. JAMA 2012;308:1237–45.

64. Taylor CA, Fonte TA, Min JK. Computational fluid dynamics applied to cardiac computed tomography for noninvasive quantification of fractional flow reserve: scientific basis. J. Am. Coll. Cardiol. 2013;61:2233–41.

65. Norgaard BL, Leipsic J, Gaur S, et al. Diagnostic performance of noninvasive fractional flow reserve derived from coronary computed tomography angiography in suspected coronary artery disease: the NXT trial (Analysis of Coronary Blood Flow Using CT Angiography: Next Steps). J. Am. Coll. Cardiol. 2014;63:1145–55.

66. Murthy VL, Bateman TM, Beanlands RS, et al. Clinical Quantification of Myocardial Blood Flow Using PET: Joint Position Paper of the SNMMI Cardiovascular Council and the ASNC. J. Nucl. Cardiol. 2018;25:269–97.

67. Murthy VL, Naya M, Foster CR, et al. Association between coronary vascular dysfunction and cardiac mortality in patients with and without diabetes mellitus. Circulation 2012;126:1858–68.

68. Ceyrat Q, Bordenave L, Couffinhal T, Douard H, Debordeaux F, Pinaquy JB. Évaluation quantitative de la réserve coronaire avec les caméras CZT, faisabilité et perspectives. Médecine Nucléaire 2019;43:185.

69 . Ceyrat Q, Bordenave L, Couffinhal T, Douard H, Debordeaux F, Pinaquy JB. Evaluation quantitative de la réserve coronaire avec les caméras CZT, faisabilité et perspectives. Médecine Nucléaire 2019;43:185

Figure 1

Resting and hyperemic myocardial blood flow (MBF) according to the presence/absence of flow-limiting coronary stenosis (CFR).

Flux sanguin myocardique au repos et en situation d'hyperémie selon la présence/absence d'une sténose coronaire limitant le flux sanguin

Figure 2

Cardiovascular mortality according to MBF and CFR. Adapted from Gupta et al. [8].

Mortalité cardiovasculaire en fonction du flux sanguin myocardique et de la réserve coronaire. Adapté de Gupta et coll.

Figure 3

Example of ^{82}rubidium positron emission tomography myocardial perfusion imaging (^{82}Rb-PET-MPI). ^{82}Rb-PET-MPI in a 62-year-old man with chest pain and positive stress electrocardiography. Stress ^{82}Rb-PET-MPI acquired during pharmacological stress (dipyridamole: 0.7 mg.kg^{-1}) showed moderate LV dilatation, lack of increased left ventricular ejection fraction during the stress and a discrete right ventricular signal associated with low global stress myocardial blood flow and myocardial flow reserve in favor of balanced myocardial ischemia. Coronary angiography confirmed the presence of 3-vessel CAD.

Exemple d'imagerie de perfusion myocardique par tomographie par émission de positrons ^{82}Rubidium. Tomographie par émission de positrons au ^{82}Rubidium : imagerie de la perfusion myocardique chez un homme de 62 ans avec des douleurs thoraciques suspectes et un stress électriquement positif. L'imagerie de perfusion TEP-Rb acquise pendant le stress pharmacologique (dipyridamole : 0,7 mg/kg) montre une dilatation modérée du ventricule gauche, l'absence d'augmentation de la fraction d'éjection du ventricule gauche au cours du

stress et un léger signal au niveau du ventricule droit associé à un faible débit sanguin myocardique global de stress et à une réserve coronaire en faveur d'une ischémie myocardique équilibrée. La coronarographie a confirmé la présence d'une coronaropathie tritronculaire chez ce patient.

Figure 4

Myocardial blood flow quantification by dynamic ^{99m}Tc-sestamibi cadmium-zinc telluride single photon emission computed tomography.

Quantification du débit sanguin myocardique par tomographie par émission monophotonique dynamique au ^{99m}Tc-sestamibi sur caméra de tellurure de cadmium-zinc

Figure 5

Principle of fractional flow reserve assessment. CFR: coronary flow reserve; FFR: fractional flow reserve. In this case, the coronary stenosis (Pd) value obtained after maximal hyperemia is 70 mmHg; the FFR value is therefore 70/100 = 0.7

Principe de l'évaluation de la réserve de flux fractionnaire. Dans ce cas, la valeur de Pd obtenue après une hyperémie maximale est de 70 mmHg ; la valeur de FFR est donc de 70 mmHg : 70/100 = 0,7

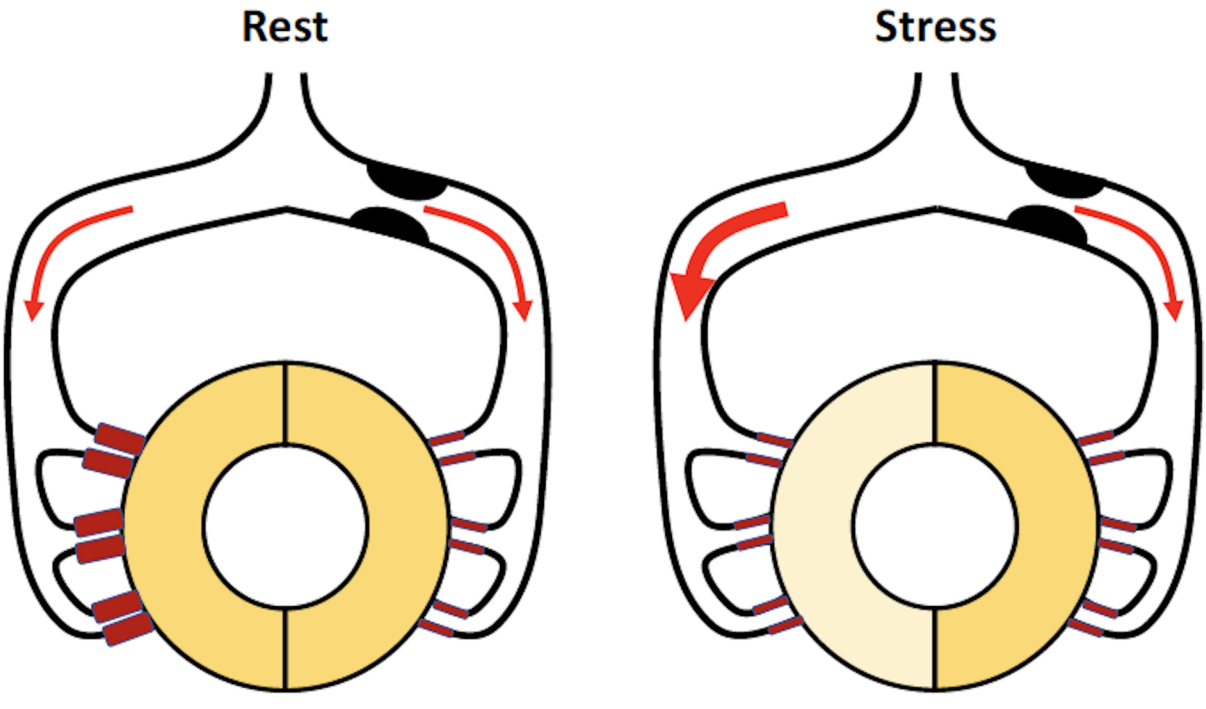
Rest
Stress

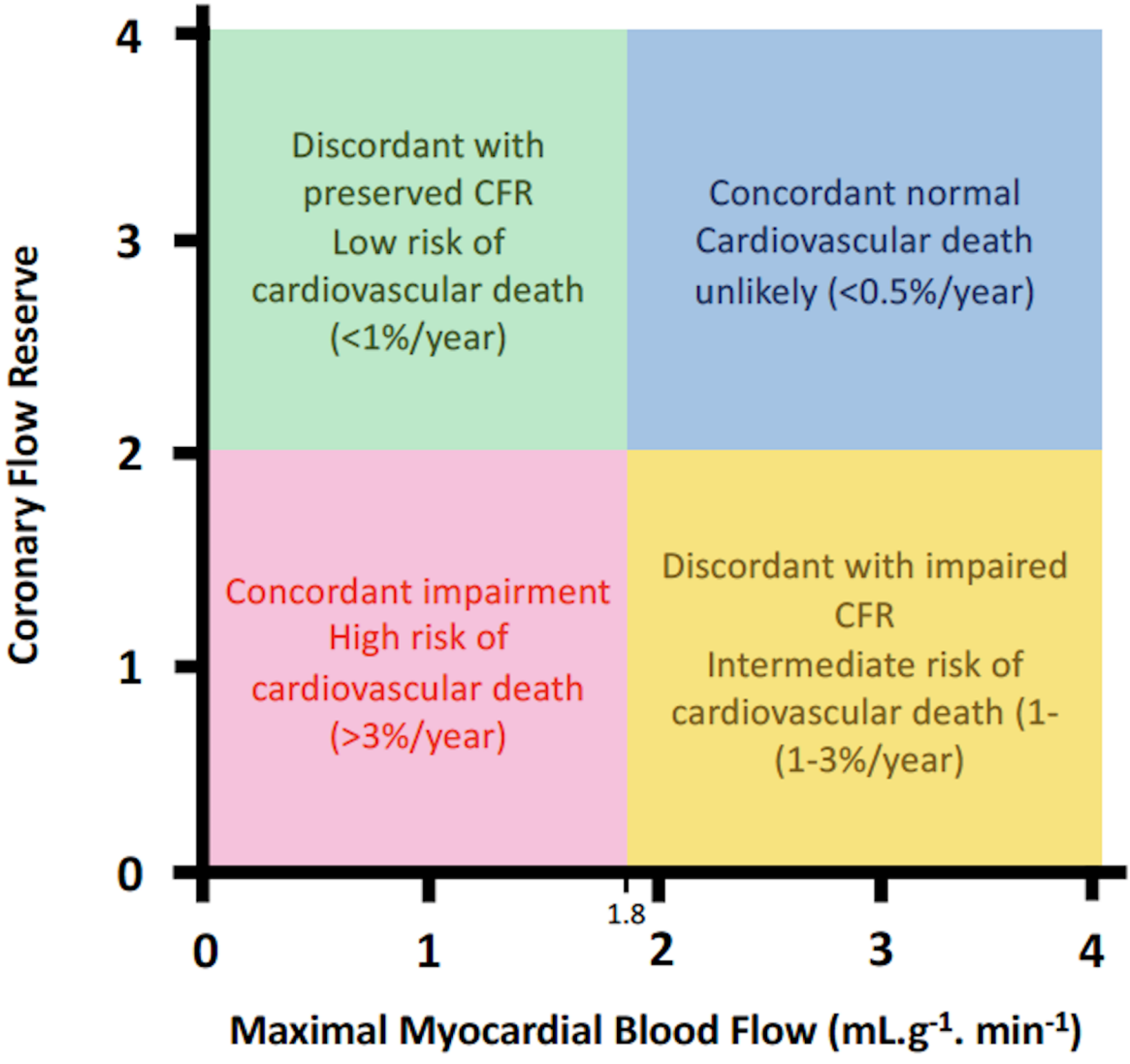
Discordant with preserved CFR
Low risk of cardiovascular death (<1%/year)
Concordant normal
Cardiovascular death unlikely (<0.5%/year)
Concordant impairment
High risk of cardiovascular death (>3%/year)
Discordant with impaired CFR
Intermediate risk of cardiovascular death (1-
(1-3%/year)
Coronary Flow Reserve
0
1
2
3
4
1.8
Maximal Myocardial Blood Flow (mL.g-1. min-1)

PET-MPI

Stress

Rest

Stress

Rest

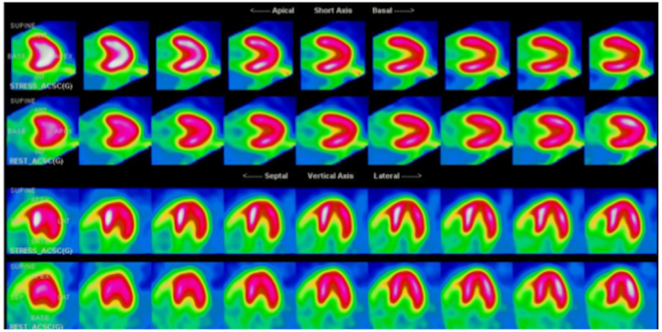

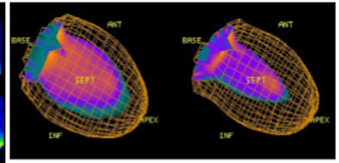

Stress

LV TD Vol. = 77 ml

LV TS Vol. = 31 ml

LVEF = 60 %

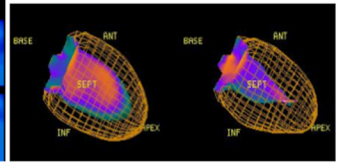

Rest

LV TD Vol. = 60 ml

LV TS Vol. = 22 ml

LVEF = 63 %

stressRubidium Flow

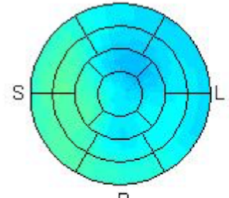

	LV	LAD	LCX	RCA
Mean	1.12	1.11	1.04	1.21
%max	85.1	84.6	79.3	91.7

restRubidium Flow

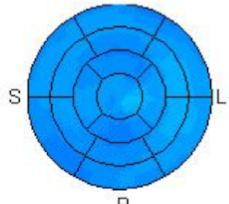

	LV	LAD	LCX	RCA
Mean	0.80	0.80	0.83	0.77
%max	94.6	94.5	98.1	91.3

stressRubidium / restRubidium

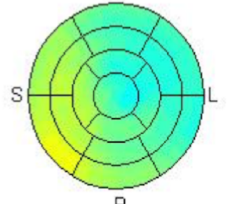

	LV	LAD	LCX	RCA
Mean	1.40	1.39	1.26	1.56
%max	80.7	80.2	72.4	89.9

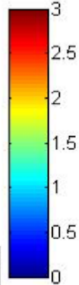

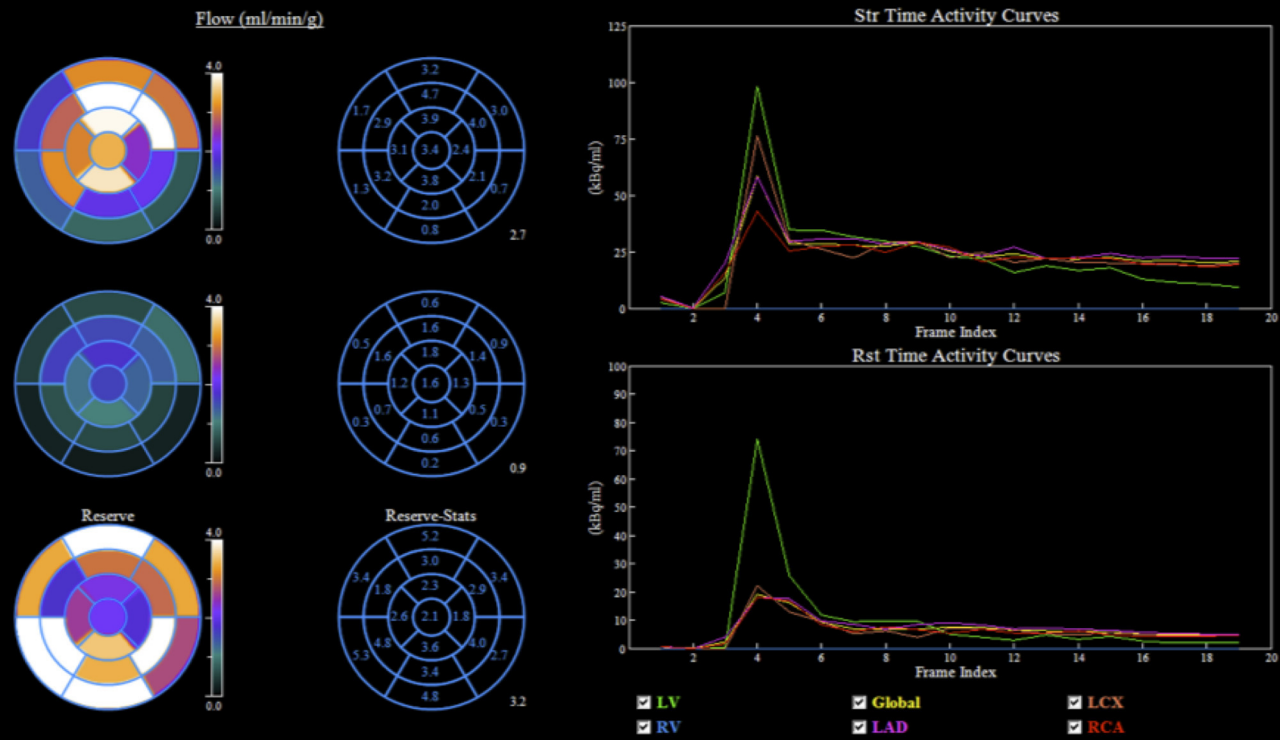
Flow (ml/min/g)
4.0
0.0
3.2
4.7
3.9
1.7
2.9
4.0
3.0
3.1
3.4
2.4
3.2
3.8
2.1
1.3
0.7
2.0
0.8
2.7
4.0
0.0
0.6
1.6
1.8
0.5
0.9
1.6
1.4
1.2
1.6
1.3
0.7
1.1
0.5
0.3
0.3
0.6
0.2
0.9
Reserve
4.0
0.0
Reserve-Stats
5.2
3.0
3.4
2.3
3.4
1.8
2.9
2.6
2.1
1.8
4.8
3.6
4.0
5.3
2.7
3.4
4.8
3.2
Str Time Activity Curves
125
100
75
50
25
0
(kBq/ml)
2
4
6
8
10
12
14
16
18
20
Frame Index
Rst Time Activity Curves
100
90
80
70
60
50
40
30
20
10
0
(kBq/ml)
2
4
6
8
10
12
14
16
18
20
Frame Index
LV
Global
LCX
RV
LAD
RCA

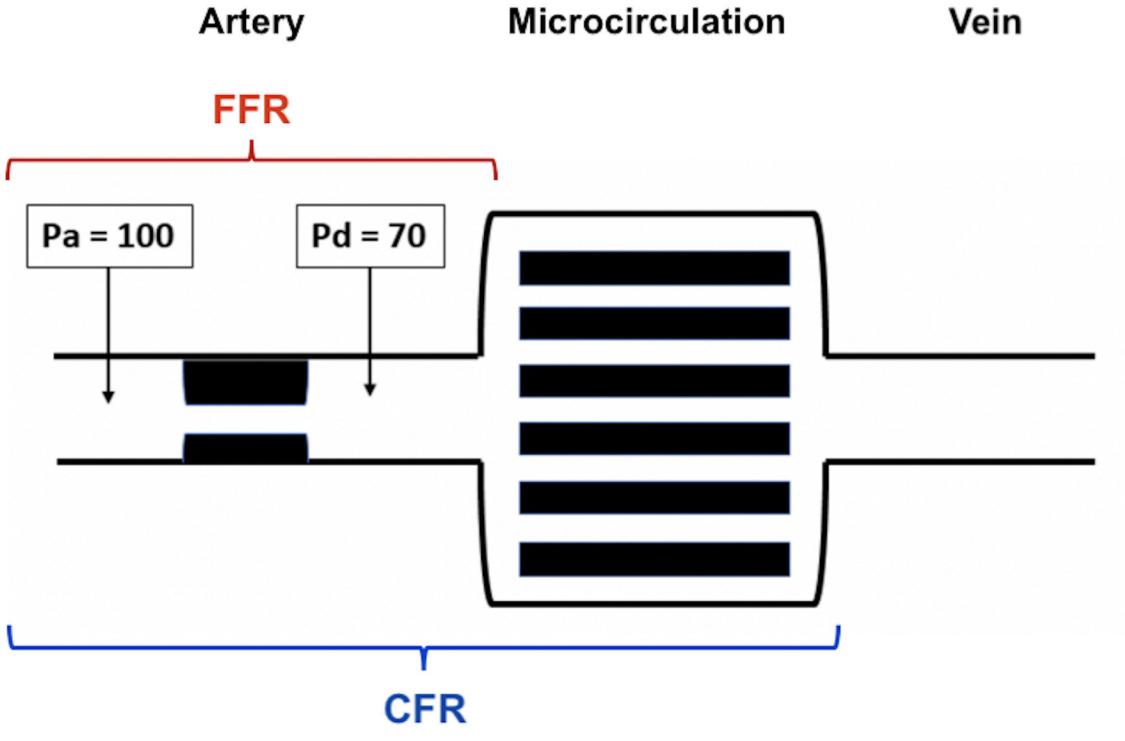
Artery
Microcirculation
Vein
FFR
Pa = 100
Pd = 70
CFR